

Methodological Principles of T Wave Alternans Analysis: A Unified Framework

Juan Pablo Martínez* and Salvador Olmos, *Member, IEEE*

Abstract—Visible T wave alternans (TWA) in the electrocardiogram (ECG) had been regarded as an infrequent phenomenon during the first 80 years of electrocardiography. Nevertheless, computerized analysis changed this perception. In the last two decades, a variety of techniques for automatic TWA analysis have been proposed. These techniques have allowed researchers to detect nonvisible TWA in a wide variety of clinical and experimental conditions. Such studies have recently shown that TWA is related to cardiac instability and increased arrhythmogenicity. Comparison of TWA analysis methods is a difficult task due to the diversity of approaches. In this paper, we propose a unified framework which holds the existing methods. In the light of this framework, the methodological principles of the published TWA analysis schemes are compared and discussed. This framework may have an important role to develop new approaches to this problem.

Index Terms—Detection, estimation, framework, T wave alternans.

I. INTRODUCTION

T-WAVE ALTERNANS (TWA), also called repolarization alternans, is a phenomenon appearing in the electrocardiogram (ECG) as a consistent fluctuation in the repolarization morphology on an every-other-beat basis. Since the first cases of TWA reported at the beginning of the 20th century [1], [2], the interest for this phenomenon has continued in the subsequent decades [3]–[5], but it was generally considered as a rare finding. It was not until the 1980s, when Adam *et al.* measured nonvisible (microvolt-level) alternans with the aid of a computer [6]–[8], that subtle TWA was shown to be much more common than visible TWA.

Since then, TWA has been related to electrical disorder and high risk of sudden cardiac death during pacing [9], stress tests [10], coronary angioplasty [11] or ambulatory recordings [12], associated with a wide range of pathological conditions such as long QT syndrome (LQTS) [13], myocardial ischemia [12], infarction [14], Prinzmetal angina [15], dilated cardiomyopathy [16] and others [17]. It has also been found in some healthy subjects, always at elevated heart rate [18]–[20].

Manuscript received January 15, 2004; revised August 29, 2004. This work was supported in part by grants TEC2004-05263-C02-02/TCM from Ministerio de Ciencia y Tecnología (Spain), PI04/0689, PI04/1795 from Fondo de Investigaciones Sanitarias and P075/2001 from Autonomous Government of Aragon. Asterisk indicates corresponding author.

*J. P. Martínez is with the Communications Technology Group, Aragon Institute of Engineering Research, University of Zaragoza. María de Luna, 1, 50018 Zaragoza, Spain (e-mail: jpmart@unizar.es).

S. Olmos is with the Communications Technology Group, Aragon Institute of Engineering Research, University of Zaragoza. 50018 Zaragoza, Spain.

Digital Object Identifier 10.1109/TBME.2005.844025

In the last two decades, a variety of analysis methods have been proposed to automatically detect and estimate TWA in the ECG [9], [17], [21]–[33], ranging from the widely-used spectral method to some recently presented nonlinear methods. In the cited references, methods are described as a concatenation of procedures (filters, transforms, decision rules, ...). The performance of such procedures depends on design parameters and heuristic rules, which are usually not optimized, but selected ad-hoc from the designer's experience. This fact, together with the diversity of approaches, make comparison of methods a difficult task.

The need for a methodological systematization effort is, thus, established. A unified framework valid for all existing methods but general enough to hold other possible approaches would permit proper characterization and comparison of each method's constituting stages, allowing the explanation of the observed performance differences. The conclusions would be then generalizable, providing valuable and solid information for future algorithm design.

We are not aware that such effort has been done up to now. Whereas the published TWA literature contains extensive reviews on TWA physiological mechanisms [34], [35] and clinical impact [36]–[40], only brief reviews of the first published methods can be found on the methodological side [36]–[38], [41]. They include some discussion about their performance, based on published results obtained under heterogeneous conditions. Other works, such as [23], [27], [42] perform a direct comparison of different methods over the same clinical or simulated dataset, but they do not tackle the problem of parameter choice.

This paper aims to provide a methodological overview of the different approaches to TWA analysis and is outlined as follows: In Section II, a brief historical panorama of TWA methods is depicted. In Section III, we establish a unified framework for TWA analysis. Section IV is dedicated to review, compare and discuss the implementations of each of the stages of the proposed general structure. Finally some considerations about validation are expressed in Section V, and conclusions are given in Section VI.

II. A HISTORICAL OVERVIEW OF TWA ANALYSIS METHODS

We present next the different approaches which, to our knowledge, have been proposed for automatic TWA analysis.

1) *The Beginnings; Energy Spectral Method (ESM)*: The first quantitative studies relating TWA with myocardial instability were published by Adam *et al.* in 1981–1984 [6]–[8]. The underlying idea was that alternans is usually observed as a 0.5 cycles-per-beat (cpb) fluctuation in the beat-to-beat measured T wave energy. TWA magnitude was measured as

the periodogram evaluated at 0.5 cpb of the normalized T wave energy series minus an estimate of the spectral background noise.

2) *Spectral Method (SM)*: The SM was proposed in 1988 by Smith *et al.* [17] as a more elaborated version of the ESM. In the SM, digitized ECG beats are aligned, and periodogram-based power spectral estimates are computed for each sample in the segment of interest. The value of an aggregate spectrum at 0.5 cpb is compared with the spectral noise level to decide if TWA is present. A slightly modified version was presented by the same group in 1994 [9]. Since then, it has been extensively used for clinical research [16], [43]–[46]. It is included in commercial equipments, such as CH2000 and Heartwave (Cambridge Heart Inc, Bedford, MA).

3) *Complex Demodulation Method (CD)*: The CD was presented in 1991 by Nearing and Verrier [21] as an alternative to the SM, allowing dynamic tracking of TWA. A more detailed description was given in [22]. In this method, the beats are also aligned, and TWA is modeled in each series as a sinusoidal signal of frequency $f = 0.5$ cpb and variable amplitude and phase. TWA amplitude in each beat-to-beat series is estimated by demodulation of the 0.5-cpb component. This method has been used in several clinical studies during ischemia [12], [47].

4) *Correlation Method (CM)*: A rather different time-domain approach to TWA analysis was proposed by Burattini and coworkers in 1997 [23]–[25]. Two main differences arise with respect to the previous ones: a) the ST-T complex is jointly analyzed, reducing all the available information in each beat to a single cross-correlation coefficient, and b) the single beat-to-beat series of coefficients is analyzed using a time-domain zero-crossing counter. The CM has been used to study TWA in coronary artery disease and LQTS [48].

5) *Karhunen-Loève Transform (KLT)*: The truncated KLT has been used to compact the energy of the ST-T complex in a reduced number of coefficients. Two proposals have made use of this transform: the first method, by Laguna *et al.* [26] in 1996, reduced each ST-T complex to the first four coefficients of the KLT. Then, each beat-to-beat series of coefficients was spectrally analyzed by means of the periodogram (KLSM). This method was tested in ambulatory ischemia records [26]. The KLT was also used by our group in 2000 [27], but analyzing the resulting coefficient series by means of complex demodulation (KLCD).

6) *Capon Filtering Method (CF)*: CF was also proposed in [27] as a variant of the CD. In CD, an *a priori* designed low-pass filter is used to discern the demodulated alternant component from nondesired components. In CF, a FIR filter that minimizes the power of the output signal while preserving the alternant component is applied instead of an invariant low-pass filter. The optimal Capon filter depends on the autocorrelation function of the input signal [49].

7) *Poincaré Mapping Method (PM)*: Poincaré Maps are used to analyze dynamic systems showing periodicity. In 2002, this technique was proposed for TWA analysis by Strumillo and Ruta [28]. For each sample in the ST-T complex, a Poincaré map is obtained by representing pairs of consecutive beat-to-beat differences in the phase space. Alternans is identified when two clusters of points are present in the Poincaré

maps and is measured in terms of the distance between the centroids of even and odd points.

8) *Periodicity Transform Method (PT)*: Srikanth *et al.* [29] proposed in 2002 a new approach for TWA detection based on the Periodicity Transform [50]. The technique is applied to the beat-to-beat series of some T wave features, such as peak amplitude, area or variance. This method computes the energy of the orthogonal projection of each series in the subspace of sequences with 2-beat periodicity.

9) *Statistical Tests Method (ST)*: The same authors presented, also in 2002, an alternative approach based on three statistical tests [30]: Student's *t* tests for independent and paired samples to test the differences between T wave features in odd and even beats, and Rayleigh's test for periodicity.

10) *Modified Moving Average Method (MMA)*: In 2002, MMA was proposed by the authors of CD as a more robust analysis approach [31]. The time-domain analysis procedure consists of continuously computing a recursive running average of odd and even beats, where a limiting nonlinearity is applied to the innovation of every new beat to avoid the effect of impulsive artifacts. Since its publication, it has been used to assess risk in post myocardial infarction patients [14] and in patients with implantable cardioverter defibrillators [20]. It is included in commercial equipment such as CASE-8000 (GE Medical Systems, Milwaukee, WI).

11) *Laplacian Likelihood Ratio Method (LLR)*: In 2002, we presented a detection theoretical approach to TWA detection [32], [33]. Given a signal model including alternans and noise terms, the maximum likelihood estimator (MLE) and the generalized likelihood ratio test (GLRT) [51] can be derived for alternans estimation and detection, respectively. The physiological noise was shown to be leptokurtic: that is, the tails of the distribution are heavier than those of a normal distribution, and therefore, we proposed a Laplacian noise model. The MLE and GLRT for this model are based on median filters. In [33] the model was extended to account for nonstationary noise. The LLR has been used to robustly detect TWA in patients undergoing coronary angioplasty [52].

12) *Other Proposals*: Besides the earlier reported methods, Nearing and Verrier also mentioned in 1996 [36], [53] estimation-by-subtraction, least squares estimation and parametric spectral estimation (AR and ARM) as possible techniques for TWA analysis, but their implementation has not been reported.

III. GENERAL STRUCTURE

A TWA analysis system can be dissected into three stages: preprocessing, data reduction and the TWA analysis proper, which can be further decomposed into the detection and estimation substages. This scheme is represented in Fig. 1. The input to the system is the digitized ECG signal. The possible outputs include the decision whether TWA is present (hypothesis \mathcal{H}_1) or absent (hypothesis \mathcal{H}_0), the TWA amplitude V_l and the alternant waveform $a_l[n]$ computed at l th beat.

A. Preprocessing

The aim of this stage is to condition the acquired ECG for posterior analysis. As TWA is a beat-to-beat phenomenon and

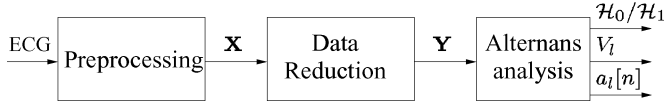


Fig. 1. General structure of a TWA analyzer. $\mathbf{X} = \{x_i[n]\}$: preprocessed segment matrix, $\mathbf{Y} = \{y_i[p]\}$: reduced coefficient matrix. $\mathcal{H}_0/\mathcal{H}_1$: decision about absence/presence of alternans. V_l : TWA amplitude. $a_l[n]$: alternant waveform.

is associated with the cardiac repolarization (ST-T complex), an alignment and segmentation procedure must be defined. QRS detection and ST-T complex segmentation are, therefore, necessary tasks. Also in this stage, the signal quality can be enhanced by filtering the signal. The output of the preprocessing stage is an $N \times M$ matrix of filtered ECG segments $\mathbf{X} = [\mathbf{x}_0, \dots, \mathbf{x}_{M-1}]$, where $\mathbf{x}_i = [x_i[0], \dots, x_i[N-1]]^T$ is the preprocessed repolarization interval (ST-T complex) of the i th beat and M is the total number of beats. The rows of \mathbf{X} are beat-to-beat series of samples with the same latency in the repolarization interval. The number of samples N of each segment $x_i[n]$ depends on the sampling frequency, the heart rate and the segmentation criterion (usually the whole ST-T complex).

B. Data Reduction

The purpose of this stage is to reduce the number of beat-to-beat series to be processed while preserving information about TWA. This can be done by removing redundancies in the signal. Note that the signal of interest, which is the possible alternant waveform in \mathbf{x}_i , is mostly concentrated between 0.3 Hz and 15 Hz [53].

A data reduction transformation $\mathbf{y}_i = \mathbf{f}(\mathbf{x}_i)$ is applied to each segment \mathbf{x}_i , where $\mathbf{y}_i = [y_i[0], \dots, y_i[P-1]]^T$ is the $P \times 1$ reduced coefficient vector ($P \leq N$) of the i th segment. The output of the stage is the $P \times M$ matrix $\mathbf{Y} = [\mathbf{y}_0, \dots, \mathbf{y}_{M-1}]$. In some cases, no data reduction is performed and $\mathbf{Y} = \mathbf{X}$.

C. TWA Analysis

In the last stage, the transformed matrix \mathbf{Y} is analyzed to decide about the presence or absence of TWA, and where appropriate, to estimate its amplitude. We can, therefore, distinguish the detection and estimation substages (Fig. 2).

Due to the transient, nonstationary nature of TWA, detection and estimation must involve a limited set of neighbor beats. Thus, we can speak of an L -beat analysis window, which must be shifted in order to cover the whole signal. Let D be the shift (in beats) of the window between two consecutive steps. Then, detection statistics and estimators will be computed every D beats. The analysis can be performed on nonoverlapping ($D = L$) or overlapping blocks ($D \leq L$), whose extreme case is the beat-by-beat sliding window analysis ($D = 1$).

1) *TWA Detection*: To decide between hypotheses \mathcal{H}_1 and \mathcal{H}_0 , a detection statistic Z_l is computed in the neighborhood of the l th beat (where $l = l_0 + rD$), quantifying the significance of the alternant component. Then, a decision rule is applied, consisting of comparing Z_l with a threshold $\gamma_Z(l)$, either fixed or variant

$$Z_l \underset{\mathcal{H}_0}{\overset{\mathcal{H}_1}{\geq}} \gamma_Z(l). \quad (1)$$

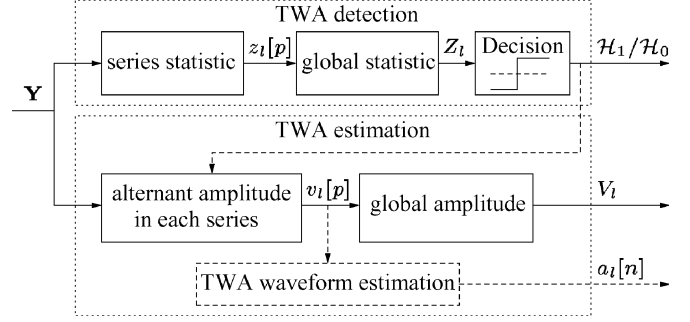


Fig. 2. Block diagram of the TWA analysis stage (see text for notation).

When $P > 1$, a set of P individual statistics $z_l[p]$ is usually computed, quantifying alternans in each row of matrix \mathbf{Y} . The global statistic Z_l summarizes the individual statistics $z_l[p]$ (e.g., through the RMS value, mean, maximum value, ...).

2) *TWA Estimation*: When alternans is detected, this substage provides an estimate of TWA amplitude.

The alternant amplitude is first estimated in each beat-to-beat coefficient series. Let $v_l[p]$ be the estimate for the p th coefficient. A global TWA amplitude V_l (in voltage units) is computed as a function of $\{v_l[p]\}_{p=0}^{P-1}$.

Note that the alternant amplitude is defined by some authors as the difference between an alternating value and the center of the fluctuation (e.g., [9] and [37]), and by others as the difference between two consecutive beats, which is exactly the double (e.g., [21] and [25]). In this paper, we will use the later definition, which provides a more true-to-life measurement, since there is no physiological significance in the average of the alternating beats.

Additionally, some methods allow the estimation of the TWA waveform ($\mathbf{a}_l = [a_l[0], \dots, a_l[N-1]]^T$), describing the distribution of TWA amplitude during the ventricular repolarization interval.

IV. METHODOLOGICAL REVIEW

In this section, the existing approaches to TWA analysis are reviewed, compared and discussed in the light of the three-stage unified framework given in the previous section (Fig. 1), giving emphasis to the similarities and differences of the various methods. Implementation details nonrelevant for discussion and comparison are omitted in the text. The reader can find more information in Tables I–III as well as in the cited references. The terminology and notation used by other authors have been adapted to the ones in Section III. Additional explanations are provided when identification with original notation is not clear.

A. Preprocessing Stage

A general preprocessing scheme is shown in Fig. 3. Table I summarizes synoptically the most relevant implementation details of the preprocessing stage. Some authors do not give details of the preprocessing stage [28]–[31], probably because the tasks performed are not specific for TWA analysis. In fact, most of the design parameters are constrained by the available equipment and the acquisition circumstances (ambulatory, stress, pacing, ...) and cannot, therefore, be considered as part of any particular

TABLE I
SYNOPTIC TABLE OF PREPROCESSING AND SEGMENTATION STAGE IMPLEMENTATIONS (N.S.: NOT SPECIFIED)

Method	F_s (Hz)	Linear filtering	Baseline wander	QRS detection	Beat rejection
ESM [8]	360	0.125-68 Hz	N.S.	N.S.	N.S.
SM [17]	1000	DC-360 Hz	block interpolation	2-stage matched filter	anomalies rejection
SM [9]	500	0.01-100 Hz	N.S.	N.S.	ectopic substitution
CD [21]/ [22]	500	DC-50Hz +notch	zero-padded FIR filter	N.S.	premature beats rejection
CM [24]/ [25]	1000	DC-60 Hz	Cubic splines	interpolated derivative	unstable RR rejection
KLSM [26]	250	No	Cubic splines	Aristotle [54]	No
KLCD [27]	250	No	Cubic splines	Aristotle [54]	No
CF [27]	250	No	Cubic splines	Aristotle [54]	No
PM [28]	500	notch 50 Hz	yes (N.S.)	wavelet transform	ectopic/noisy substitution
PT [29]	250			N.S.	
ST [30]	250			N.S.	
MMA [31]	500	DC-50 Hz	Cubic splines	N.S.	ectopic/noisy rejection
LLR [32]/ [33]	250/500	No	Cubic splines	Aristotle [54]	Not necessary

Method	Segmentation window	Alignment	Segment matrix filtering
ESM [8]	ST-T (variable)	N.S.	No
SM [17]	QRS (150 ms) and ST-T (225 ms)	QRS	No
SM [9]	QRS, ST and T (fixed)	QRS	No
CD [21]/ [22]	ST-T (230 ms)	QRS	row-wise high-pass (0.2-0.5 cpb),
CM [24]/ [25]	ST-T (RR-adjusted)	ST-T alignment	row-wise stop-band (0.1-0.35 cpb)
KLSM [26]	ST-T complex (N.S.)	QRS	No
KLCD [27]	ST-T (300 ms)	QRS	No
CF [27]	ST-T (300 ms)	QRS	No
PM [28]	ST-T (RR-adjusted)	QRS	No
PT [29]	ST-T (N.S.)	N.S.	No
ST [30]	ST-T (N.S.)	N.S.	No
MMA [31]	ST-T (N.S.)	N.S.	No
LLR [32]/ [33]	ST-T (300 ms)	QRS	column-wise low-pass (DC-15 Hz)

TABLE II
DATA REDUCTION STAGE IMPLEMENTATIONS

Method	reduction technique	N	P
ESM [8]	T wave energy	variable	1
SM [17]	Decimation	225 (ST-T)	75
SM [9]	None (Identity)	75 (T wave)	75
CD [21]/ [22]	subsegment areas	115	23
CM [24]/ [25]	template correlation	variable	1
KLSM [26]	KL transform	N.S.	4
KLCD [27]	KL transform	75	4
CF [27]	None (Identity)	75	75
PM [28]	Decimation	variable	7
PT [29]	T wave peak amplitude,	N.S.	1
ST [30]	T wave area, subsegment variances	N.S.	1
MMA [31]	Decimation	N.S.	N.S.
LLR [32]/ [33]	Decimation	75 / 150	30

method. The requirements of this stage may also be increased or relaxed depending on the robustness of subsequent stages.

1) *Digitized ECG Signal*: The electrical potentials measured at the body surface must be converted into digital signals. The characteristics of the acquisition equipment, i.e., sampling rate, amplitude resolution, and frequency response, set a limit on the signal quality, influencing, therefore, the analysis performance.

The sampling rates F_s used in the literature range from 250 to 1000 Hz (Table I). With any of them, the main ECG components are well preserved [55]. In [56], it was concluded that TWA amplitude estimates (using the CM) were essentially identical for sampling rates in the range 250–1000 Hz, observing only slight differences when sampling at 100 Hz.

TABLE III
SUMMARY OF THE ANALYSIS STAGE OF TWA METHODS AND SOME OF THEIR DISCUSSED FEATURES (N.S.: NOT SPECIFIED)

Method	L (beats)	D (beats)	technique	estimation $V_l / a_l[n]$
ESM [8]	1024	1024	periodogram	no / no
SM [17]	128	128	modified periodogram	yes / yes**
SM [9]	128	128	periodogram	yes / yes**
CD [21]/ [22]	~30 *	1	complex demodulation	yes / yes
CM [24]/ [25]	7	1	zero-crossing counting	yes / no
KLSM [26]	5 min.	$L/2$	periodogram	no / no
KLCD [27]	16	1	complex demodulation	yes / yes
CF [27]	10	1	capon filtered CD	yes / yes
PM [28]	100	100	Poincaré mapping	yes / yes
PT [29]	16	1	periodicity transform	no / no
ST [30]	32	1	hypothesis tests	no / no
MMA [31]	~9 *	1	non-linear moving average	yes / yes
LLR [32]/ [33]	32	1	GLRT (median-based)	yes / yes

* For comparison purposes the equivalent length of the impulse response

$L = \sum h_{1pf}^2[n] / \max(h_{1pf}^2[n])$ is given for methods based in IIR filters.

** The SM allows estimation of the absolute value of the TWA waveform.

The amplitude resolution determines the accuracy of TWA measurements. From the methodological side, the lack of resolution can be characterized as an additive *quantization noise*. Current 12-bit and 16-bit analog-to-digital converters allow resolutions from 0.6 μV to 2.4 μV (for a dynamic range of ± 5 mV), clearly lower than other noise sources in most acquisition conditions.

The frequency response of different ambulatory ECG recorders was quantified by Nearing *et al.* [53], concluding

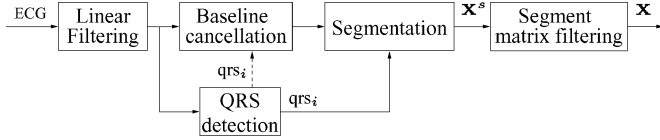


Fig. 3. General preprocessing stage. $\mathbf{X}^s = \{x_i^s[n]\}$: beat-to-beat repolarization matrix. $\mathbf{X} = \{x_i[n]\}$: filtered repolarization matrix. qrs_i : i th beat QRS fiducial point.

that amplitude-modulated (AM) Holter recorders introduced heart-rate dependent distortion in the alternant component, mainly due to the “head effect” ripple. Frequency-modulated (FM) and digital recorders showed minimal distortion for heart rates in the range from 60 to 200 bpm. A bandpass response between 0.05 and 50 Hz was recommended for ambulatory TWA monitoring.

Reliable TWA analysis in conditions such as exercise test may require more sensitive acquisition techniques (use of multicontact electrodes, independent measurements for respiration and body motion compensation), as discussed in [37].

2) *Linear Filtering*: Low-pass linear filtering is used to reject out-of-band noise. In the references, the cutoff frequencies range from 50 to 360 Hz (Table I). Filters with narrower passbands could have been used as the TWA spectrum concentrates within the 0.3–15 Hz range [53]. However, QRS complexes would lose their high-frequency components, what might degrade QRS detection and alignment. Moreover, the widened QRS could invade the adjacent ST-T complex. Some references [22], [28] report the use of notch filters to cancel powerline interferences (50/60 Hz).

3) *Baseline Wander Cancellation*: Baseline fluctuations may manifest as high amplitude noise when analysing the beat-to-beat series, degrading the analysis performance (masking subtle TWA or generating false detections). Cancellation of baseline changes in the preprocessing stage is, therefore, convenient. Both filtering [22] and interpolation approaches [25]–[27] have been used in the TWA literature.

4) *QRS Detection and Segmentation*: QRS detection is an extensively studied topic in ECG signal processing [57]. In the TWA references, well-known techniques are used for this task (see Table I). Besides good detection performance, QRS detectors used for TWA analysis must show inter-beat stability in the fiducial point determination. Otherwise, the detection jitter will be transferred into the matrix \mathbf{X} as misalignment. Narayan and coworkers [58] studied this topic by using the SM with different alignment strategies. Cross-correlation with a template proved better than other strategies based on threshold crossing or peak location.

A later alignment of ST-T complexes, maximizing their cross-correlation with a template, was performed in [24]. Although this approach reduces the effect of detection jitter, it also attenuates TWA since odd and even complexes are aligned to the same template, as it was verified by Narayan *et al.* [58] for the SM.

The criteria to define the segments of interest are diverse. In most methods, the ST-T complex is selected with a fixed [9], [17], [21], [22] or RR-adjusted time window [24], [25], [28] relative to the QRS position. Some works analyze separately the ST segment and the T wave [9] or even include

the QRS complex [9], [17]. The raw ECG is then mapped into the $N \times M$ segment matrix $\mathbf{X}^s = [\mathbf{x}_0^s, \dots, \mathbf{x}_{M-1}^s]$, where $\mathbf{x}_i^s = [x_i^s[0], \dots, x_i^s[N-1]]^T$ is the i th beat selected segment.

In most methods, beats and signal excerpts not suitable for subsequent analysis are rejected. The rejection criteria include premature or ectopic beats, RR instability and bad signal quality. Rejection is crucial in TWA analysis methods not dealing well with impulsive noise (see Section IV-E), while robust methods, as the MMA or LLR, can be more tolerant at this stage. The rejected beats can be either directly eliminated or replaced by a template. The effect of beat deletion and substitution within a TWA episode in the SM has been discussed in [37], [58].

5) *Segment Matrix Filtering*: Column-wise filtering of the aligned segment matrix \mathbf{X}^s combines samples within the same ST-T complex. In the LLR [32], [33], \mathbf{X}^s was column-wise smoothed with a low-pass filter (cutoff frequency 15 Hz) in order to reject noise out of the TWA band. The problems of QRS distortion and energy spreading were circumvented by filtering the segment matrix \mathbf{X}^s instead of the raw ECG.

Row-wise filtering combines samples with the same latency in different beats. Thus, it can be used to discriminate beat-periodic components (such as dc, respiration, physiologic variability) in the *beatquency* domain [59] (measured in cpb). In CD and LLR approaches a detrending filter is applied to the rows of \mathbf{X}^s so as to remove the dc and low-frequency fluctuations. Similarly, the CM filters the rows of \mathbf{X}^s with a linear stop-band filter to cancel amplitude modulation due to respiration [25].

B. Data Reduction

Only the information preserved in this stage will be accessible to the analysis stage. It is, therefore, important that alternans in the ST-T complex is well represented in the reduced coefficients $y_i[p]$.

When the characterization of the TWA temporal distribution (the alternant waveform) is contemplated, the transformed coefficients $y_i[p]$ must provide an adequate representation of the repolarization waveform (e.g., by means of decimation, linear expansions, etc.). If the data reduction transformation $\mathbf{y}_i = \mathbf{f}(\mathbf{x}_i)$ is linear, it can be written as

$$\mathbf{y}_i = \mathbf{T}^T \mathbf{x}_i. \quad (2)$$

The ST-T complex represented by \mathbf{y}_i can then be denoted by

$$\hat{\mathbf{x}}_i = \mathbf{T}(\mathbf{T}^T \mathbf{T})^{-1} \mathbf{y}_i = \mathbf{T}(\mathbf{T}^T \mathbf{T})^{-1} \mathbf{T}^T \mathbf{x}_i \quad (3)$$

i.e., the projection of the preprocessed waveform \mathbf{x}_i into the column subspace of \mathbf{T} . It can be shown [60] that (3) is equivalent to a linear time variant periodic filter (LTVVPF) whose characteristics depend on \mathbf{T} . Thus, linear data reduction strategies can be interpreted as an additional filtering of the data.

Other strategies do not intend to estimate the TWA morphology and perform this stage by just selecting a representative feature of repolarization to be used for TWA detection and estimation.

The data reduction strategies found in the TWA literature can be classified according to whether the coefficients $y_i[p]$ reflect 1) time-localized or 2) global characteristics of the repolarization.

Table II summarizes these strategies, as well as their input and output dimensionalities (N and P)

1) *Time Localized Characteristics*: We include in this category transformations whose coefficients $y_i[p]$ carry temporally localized information.

a) *No data reduction*: In [9], [27], [31], and [58], the rows of the preprocessed signal \mathbf{X} are directly analyzed by the TWA analysis stage (i.e., $P = N$ and $\mathbf{y}_i = \mathbf{x}_i$). These implementations do not take advantage of the redundancy in alternans between adjacent rows (the sampling frequencies are 250 Hz [27], 500 Hz [9], [31], and 1000 Hz [58]).

b) *Decimation*: A very simple procedure for data reduction is time-domain decimation, as in the SM [17] and the PM [28]. By decimating the segments $x_i[n]$ by a factor of Q , the equivalent sampling frequency is reduced to F_s/Q . The segments must, therefore, be bandlimited to $F_s/(2Q)$ to prevent aliasing.

Provided that the cutoff frequency of the preprocessing low-pass filter is low enough, the data reduction consists of just keeping one out of Q samples of the segment: $y_i[p] = x_i[pQ]$, $p = 0, \dots, P-1$, where $P = \lfloor N/Q \rfloor$ is the number of samples of the decimated segment. Otherwise, an antialiasing low-pass filter must be used before decimation. In any case, the waveform $\hat{\mathbf{x}}_i$ represented by \mathbf{y}_i , is a low-pass filtered version of \mathbf{x}_i , with cutoff frequency $F_s/(2Q)$. The fact that the TWA energy is concentrated in a 15 Hz bandwidth [53] imposes a lower limit in the final dimension P in order not to filter the desired signal. In the literature, P ranges from 7 [28] to 75 [17]. Considering an ST-T duration of 225 ms, the equivalent cutoff frequencies are 16 Hz and 167 Hz, respectively. In both cases, this stage filters more restrictively than the preprocessing stage (see Table I) while preserving the desired signal.

c) *Subsegment areas*: Nearing and Verrier [22] reduce dimensionality in CD by dividing the segments of interest into subsegments of Q samples and computing the area enclosed between the ECG and the baseline

$$y_i[p] = \sum_{n=pQ+1}^{(p+1)Q} x_i[n], \quad p = 0 \dots P-1 \quad (4)$$

where $P = \lfloor N/Q \rfloor$. This is equivalent, up to a constant factor, to decimation by Q with a previous antialiasing running average filter of Q samples. In [22], the final segment dimension is $P = 23$ ($Q = 5$ with $F_s = 500$ Hz), resulting in an equivalent cutoff frequency of 50 Hz.

d) *Other local features*: T peak amplitude and variance in T wave subsegments have been used by Srikanth *et al.* in [29], [30]. In this cases, the signal morphology is lost and TWA waveform cannot be posteriorly estimated.

2) *Global Characteristics*: The techniques included in this group transform the ECG samples into coefficients reflecting characteristics of the whole repolarization interval.

a) *Template correlation*: The CM [24], [25] uses this approach, where each segment \mathbf{x}_i is represented by the so-called alternans correlation index

$$y_i[0] = \text{ACI}(i) = \frac{\sum_{n=0}^{N-1} x_i[n]x_{\text{med}}[n]}{\sum_{n=0}^{N-1} x_{\text{med}}^2[n]} = \frac{\mathbf{x}_{\text{med}}^T \cdot \mathbf{x}_i^T}{\|\mathbf{x}_{\text{med}}\|_2^2} \quad (5)$$

which is the normalized correlation with a template ST-T complex \mathbf{x}_{med} , computed as the median of 128 adjacent segments \mathbf{x}_i .

According to the filtering interpretation of (2) and (3), each preprocessed ST-T complex \mathbf{x}_i is projected into the rank-one subspace spanned by the normalized template $\mathbf{t}_0 = \mathbf{x}_{\text{med}}/\|\mathbf{x}_{\text{med}}\|_2$. The main problem with this approach is the mismatch between \mathbf{x}_{med} and the actual signal of interest (the alternant waveform). The underlying assumption is that the TWA morphology is similar to the ST-T complex, which does not usually hold true. Consequently, a significant fraction of the alternant energy is likely to project in the transformation null-space and will be lost. In an extreme case, the TWA would be undetectable if the alternant waveform and the median ST-T complex were orthogonal. TWA morphology is also lost in this method.

b) *Truncated orthogonal transform*: In [26] and [27], \mathbf{y}_i contains the first $P = 4$ KLT coefficients of each segment \mathbf{x}_i . The transformation matrix \mathbf{T} is then a $N \times P$ matrix whose columns \mathbf{t}_p , $p = 0, \dots, P-1$ are the P first KLT basis vectors. Each segment \mathbf{x}_i is described in this domain in terms of the correlation with the basis vectors \mathbf{t}_p . Since the first basis vectors of the KLT define the subspace containing the most dominant signal morphologies, this approach can be considered as an extension of template correlation.

The KLT basis must be estimated from a training set. While Laguna *et al.* use a *universal* training set [26] (data from ECG databases accounting for a wide range of repolarization morphologies), we used a *patient-specific* training set [27] (i.e., training beats belonging to each processed record).

The signal represented by \mathbf{y}_i is the projection into the column subspace of \mathbf{T} , $\hat{\mathbf{x}}_i = \mathbf{T}\mathbf{T}^T\mathbf{x}_i$, which is a linear time-variant filter adapted to the local frequency content of the training set dominant morphologies [60]. This approach improves the signal-to-noise ratio of the signal, since the ECG is essentially represented in the column subspace of \mathbf{T} , while a significant fraction of the noise power is not [61].

It should be noted that, similarly to the CM, the KLT basis is adapted to the dominant ST-T morphologies instead of the TWA morphologies. However, the use of a greater dimension ($P = 4$) allows to extend the scope of detectable morphologies with respect to the CM ($P = 1$), as it was shown in [27] where different simulated alternant waveforms were reconstructed with this method.

c) *Other global features*: T wave energy [8] and T wave area [29], [30] are some other global features used for TWA detection. Morphology information is lost in both cases ($P = 1$).

C. TWA Analysis: Detection

The first task of TWA analysis is to decide about the presence/absence of TWA ($\mathcal{H}_1/\mathcal{H}_0$) in the series of reduced-dimension coefficients $\{y_i[p]\}$. Table III summarizes the different techniques used in the literature for this purpose. In spite of the different proposed approaches, some of them yield similar detection statistics, as it will be shown. Consequently, we will classify the methods according to the way of computing the individual detection statistic $z_l[p]$ (or the global statistic Z_l if

$P = 1$) as belonging to one of three categories: 1) statistics related to the short-time Fourier transform (STFT) or equivalently, to high-pass linear filtering, 2) statistics based on sign-change counting, and 3) the recent nonlinear filtering methods.

1) *STFT-Based Methods*: The detection statistics of the methods in this class are computed from the normalized row-wise STFT of \mathbf{Y} (beat-to-beat series of coefficients) evaluated at 0.5 cpb

$$\begin{aligned} Y_w[p, l] &= \text{STFT}_{w, l} \{y_i[p]\} |_{f=0.5} \\ &= \sum_{i=-\infty}^{\infty} y_i[p] w[i-l] e^{-j2\pi f i} \Big|_{f=0.5} \\ &= \sum_{i=-\infty}^{\infty} y_i[p] w[i-l] (-1)^i \end{aligned} \quad (6)$$

where $w[k]$ is an L -beat analysis window. According to the filter-bank interpretation of the STFT [49], $Y_w[p, l]$ can be expressed as

$$Y_w[p, l] = (-1)^l \sum_{i=-\infty}^{\infty} y_i[p] h_{\text{hpf}}[l-i] = (-1)^l (y_l[p] * h_{\text{hpf}}[l]) \quad (7)$$

where $h_{\text{hpf}}[k] = w[-k](-1)^k$ is a high-pass linear filter.

The most widely used TWA analysis techniques (periodogram and complex demodulation) belong to this category. We will also show that other recent approaches also yield statistics based on (6)/(7), even though they are not originally related to spectral analysis or linear filtering (e.g., the Poincaré maps distance or the Student tests).

a) *Periodogram based*: Spectral methods compute the periodogram (standard or modified) to detect alternans over beat-to-beat series of samples (SM [9] and [17]), T wave energy (ESM [8]) or KL coefficients (KLSM [26]). The detection statistic is the 0.5 cpb bin of the short-time periodogram, which is proportional to the squared modulus of the STFT

$$z_l[p] = \frac{1}{L} |Y_w[p, l]|^2 \quad (8)$$

where $w[i]$ is the L -beat periodogram analysis window. The global detection statistic is the mean of the individual statistics $Z_l = (1/P) \sum_{p=0}^{P-1} z_l[p]$.

The decision rule in [9], [17] is defined in terms of a significance measure called TWA ratio (TWAR)

$$\text{TWAR}(l) = \frac{Z_l - m_l}{s_l} \quad (9)$$

where m_l, s_l are the mean and standard deviation of the spectral noise measured at a properly chosen spectral window. Note that applying a fixed threshold (typically $\gamma = 3$) to the TWAR is equivalent to applying a variable noise-dependent threshold to Z_l

$$\text{TWAR}(l) \underset{\mathcal{H}_0}{\overset{\mathcal{H}_1}{\geq}} \gamma \Leftrightarrow Z_l \underset{\mathcal{H}_0}{\overset{\mathcal{H}_1}{\geq}} \underbrace{\gamma s_l + m_l}_{\gamma z(l)}. \quad (10)$$

b) *Complex demodulation*: This spectral analysis technique is used in CD [21] and KLCD [62] methods over series

of samples and KL coefficients, respectively. The individual detection statistic is the magnitude of the low-pass filtered demodulated 0.5 cpb component

$$z_l[p] = |(y_l[p] \cdot (-1)^l) * h_{\text{lpf}}[l]| \quad (11)$$

which can be rewritten as

$$z_l[p] = |y_l[p] * h_{\text{hpf}}[l]| \quad (12)$$

where $h_{\text{hpf}}[k] = h_{\text{lpf}}[k] \cdot (-1)^k$ is a high-pass filter resulting from frequency translation of the low-pass filter. According to (7), the complex demodulation statistic (12) can be written as $z_l[p] = |Y_w[p, l]|$, with an analysis window $w[k] = h_{\text{lpf}}[-k]$. The global statistic is obtained by aggregating the individual ones ($Z_l = \sum_{p=0}^{P-1} z_l[p]$ in [22] and $Z_l = \text{RMS}(z_l[p])$ in [27]). The CD method provides a new detection statistic for each new beat.

The more sophisticated CF [27] replaces the invariant low-pass filter $h_{\text{lpf}}[k]$ by an optimal data-dependent Capon filter [49]. The optimality of the filter relies on the knowledge of the beat-to-beat autocorrelation $r_{y_l}(k) = E\{y_l[p]y_{l+k}[p]\}$. In practice, the autocorrelation must be estimated from the data, and the estimation error degrades the method performance. Thus, only slight improvement was achieved at the cost of a remarkable increase in complexity [27].

No specific decision rule was given by Nearing *et al.* in [21], [22] since TWA is considered to have a continuously changing magnitude (not just being present or absent). However, in other works [27], [42], [62] a fixed or variable threshold has been applied to the total alternans magnitude Z_l to distinguish alternans from noise.

c) *Poincaré map distance*: The detection statistic proposed by Strumillo and Ruta [28] is the distance between the centroids of even and odd groups of beats in the phase space

$$\begin{aligned} z_l[p] &= |E\{y_{2i+1}[p] - y_{2i}[p]\} - E\{y_{2i}[p] - y_{2i-1}[p]\}| \\ &\cong 2 |E\{y_{2i}[p] - y_{2i-1}[p]\}|. \end{aligned} \quad (13)$$

The expected value in (13) is estimated as the average within a window of $L = 100$ beats as

$$\begin{aligned} z_l[p] &= 2 \left| \frac{1}{L} \sum_{i=\frac{(l-L)}{2}+1}^{\frac{l}{2}} (y_{2i}[p] - y_{2i-1}[p]) \right| \\ &= \frac{2}{L} \left| \sum_{j=l-L+1}^l y_j[p] (-1)^j \right| \\ &= \frac{2}{L} |Y_w[p, l]|. \end{aligned} \quad (14)$$

The analysis window is in this case an L -beat rectangular window. The aggregated statistic Z_l is computed as the average for all the series in the ST-T complex $Z_l = (1/P) \sum_{p=0}^{P-1} z_l[p]$

d) *Projection in 2-periodicity space*: In the PT method [29] a feature series is analyzed in beat-to-beat updated blocks of $L = 16$ beats $\{y_i\}_{i=l-L+1}^l$. The average \bar{y}_l is removed of each sequence and the energy of its projection onto the space of sequences with 2-periodicity is computed as the detection

statistic. The two coefficients of the projection are given by the mean of the even and odd samples of the zero-measured sequence

$$\alpha_0(l) = \frac{2}{L} \sum_{k=0}^{\frac{L}{2}-1} (y_{l-L+2k+1} - \bar{y}_l) \quad (15)$$

$$\alpha_1(l) = \frac{2}{L} \sum_{k=0}^{\frac{L}{2}-1} (y_{l-L+2k+2} - \bar{y}_l) = -\alpha_0(l) \quad (16)$$

with $\bar{y}_l = (1/L) \sum_{k=0}^{L-1} y_{l-L+1+k}$. The detection statistic becomes $Z_l = \alpha_0^2(l) + \alpha_1^2(l) = 2\alpha_0^2(l)$. Substituting the value of \bar{y}_l in (15) it can be shown that

$$Z_l = \frac{2}{L^2} \left| \sum_{k=l-L+1}^l y_k (-1)^k \right|^2 = \frac{2}{L^2} |Y_w[0, l]|^2 \quad (17)$$

where again an L -beat rectangular window is used in the analysis.

e) Student's t-tests: Student's t test for independent and paired samples are used in the ST [30] to decide whether the differences observed between the features of the odd and even beats are significant. The analysis is performed in sequences of $L = 32$ beats updated for every new beat.

When using the standard t -test, the statistic

$$t_l = \frac{m_l^{\text{even}} - m_l^{\text{odd}}}{\frac{S_l}{\sqrt{\frac{L}{4}}}}$$

with $S_l = \sqrt{\frac{1}{2} (s_l^{\text{even}})^2 + \frac{1}{2} (s_l^{\text{odd}})^2}$ (18)

is computed where m_l^{even} , m_l^{odd} , s_l^{even} , and s_l^{odd} are the sample mean and sample standard deviation of even and odd beats, respectively. The p -value of the test is compared to a significance level (the α -level) to make the decision. Due to the monotonic relation between the p -value and $|t_l|$, this decision rule is equivalent to decide TWA if $|t_l| > \gamma$ where γ is the critical value of the test statistic for the considered α -level (e.g., $\gamma = 2.042$ for $\alpha = 0.005$ and $L = 32$ which are the values used in [30]). Then, TWA is decided if

$$\underbrace{|m_l^{\text{even}} - m_l^{\text{odd}}|}_{Z_l} \underset{\mathcal{H}_0}{\overset{\mathcal{H}_1}{\geq}} \gamma \underbrace{\frac{S_l}{\sqrt{\frac{L}{4}}}}_{\gamma_Z(l)}. \quad (19)$$

Note that $Z_l = |m_l^{\text{even}} - m_l^{\text{odd}}| = |Y_w[0, l]|$ for an L -beat rectangular analysis window.

The paired t -test is an alternative to avoid the influence of low frequency trends in the analyzed sequence which inflate the intra-group variances. In this case, couples of consecutive beats are considered to be paired. The statistic

$$t_l^\Delta = \frac{m_l^\Delta}{\frac{s_l^\Delta}{\sqrt{\frac{L}{2}}}} \quad (20)$$

where m_l^Δ , s_l^Δ are the sample mean and standard deviation of the $L/2$ differences $\Delta_i = y_{2i} - y_{2i-1}$, is used to test if the mean difference between consecutive beats is significantly different

from zero. The decision rule can again be expressed as $|t_l^\Delta| \underset{\mathcal{H}_0}{\overset{\mathcal{H}_1}{\geq}} \gamma$ or

$$\underbrace{|m_l^\Delta|}_{Z_l} \underset{\mathcal{H}_0}{\overset{\mathcal{H}_1}{\geq}} \gamma \underbrace{\frac{s_l^\Delta}{\sqrt{\frac{L}{2}}}}_{\gamma_Z(l)} \quad (21)$$

where $Z_l = |m_l^\Delta| = |Y_w[0, l]|$ is the same statistic as in the standard test.

2) Sign Change Counting Methods: The Rayleigh test (included in ST) and the CM belong to this category. Both use a strategy based on the time-domain observation of the sign changes (or zero-crossings) in a beat-to-beat series.

The Rayleigh test in [30] decides if a series can be explained either by a random distribution or by a periodic pattern by measuring the regularity of the phase reversal pattern (sign reversal pattern for 2-beat periodicity). The feature series $\{y_i\}$ is analyzed with a sliding window of $L = 32$ beats. In each data block, the number of deviations with respect to one of the two alternant patterns $\{y_i > y_{i+1}, y_{i+1} < y_{i+2}, y_{i+2} > y_{i+3}, \dots\}$ or $\{y_i < y_{i+1}, y_{i+1} > y_{i+2}, y_{i+2} < y_{i+3}, \dots\}$ is measured, and a significance value is given meaning the probability of obtaining such a pattern from a random variable. A given significance value is associated with a fixed threshold γ_Z in the number of beats following one of the patterns. Thus, \mathcal{H}_1 is decided if

$$Z_l = \frac{1}{2} \left(L + \left| \sum_{i=l-L+1}^l \text{sign}(\Delta y_i) (-1)^i \right| \right) \geq \gamma_Z \quad (22)$$

where $\{\Delta y_i\} = \{y_i - y_{i-1}\}$. Rewriting (22) as

$$Z_l = \frac{1}{2} \left(L + |\text{STFT}_{w,l} \{\text{sign}(\Delta y_i)\}|_{f=0.5} \right) \geq \gamma_Z \quad (23)$$

highlights the relation to the STFT-based methods. The STFT is now applied to the sign of the Δ_i series.

In the CM, the alternans correlation index $\{y_i\}$ (5) is usually near one, since ST-T complexes are similar to the template. However, when TWA is present, the correlation is expected to alternate between values greater and lesser than one. Burattini *et al.* [25] require $L = 7$ consecutive sign changes in the series $\{\Delta y_i\} = \{y_i - 1\}$ to decide the presence of TWA. Using our notation, the decision rule for detecting alternans is also (22) with threshold $\gamma_Z = L$.

3) Nonlinear Filtering Methods: This category includes some very recently proposed analysis methods where nonlinear filters are used to compute the detection statistics and magnitude estimates.

a) Nonlinear moving average: In the MMA method [14] an MMA is applied in parallel to even and odd beats as

$$\bar{y}_l[p] = \bar{y}_{l-2}[p] + g \left(\frac{(y_{l-2}[p] - \bar{y}_{l-2}[p])}{8} \right) \quad (24)$$

where $g(x)$ is a nonlinear limiting function

$$g(x) = \begin{cases} -K, & \text{if } x < -K \\ x, & \text{if } |x| \leq K \\ K, & \text{if } x > K \end{cases}. \quad (25)$$

The TWA at the l th beat is computed as the absolute difference between even and odd estimates

$$z_l[p] = |\bar{y}_l[p] - \bar{y}_{l-1}[p]|, \quad (26)$$

and the global detection statistic is quantified as

$$Z_l = \max_p z_l[p] = \max_p [\bar{y}_l[p] - \bar{y}_{l-1}[p]]. \quad (27)$$

b) Median-based GLRT detectors: In [32] (LLR), a GLRT detector was derived for TWA in Laplacian noise with known power. The individual statistic in each series is beat-to-beat computed as

$$z_l[p] = \frac{2\sqrt{2}}{L} \left| \sum_{i \in [l-L+1, l] \cap B} y_i[p](-1)^i \right|, \\ B = \{i; \min(0, v_l[p]) < 2y_i[p](-1)^i < \max(0, v_l[p])\}. \quad (28)$$

It is proportional to the absolute sum of the values of the demodulated series lying between 0 and the MLE of the alternant amplitude $v_l[p]$. For Laplacian noise, $v_l[p]$ is twice the median filtered demodulated series

$$v_l[p] = 2 \operatorname{median}_{i=l-L+1}^l \{y_i[p](-1)^i\}. \quad (29)$$

The global GLRT is the mean of the series statistics $Z_l = \sum_p z_l[p]/P$, and is compared to a fixed threshold.

When noise power is not assumed to be stationary [33], the resulting GLRT is equivalent to comparing the previous Z_l with a variable threshold $\gamma_Z(l) = \gamma_{s_l}$, where s_l is the MLE of the noise standard deviation under hypothesis \mathcal{H}_1 : $s_l = (\sqrt{2}/PL) \sum_i \sum_p |y_i[p] - v_l[p](-1)^i|$.

D. TWA Analysis: Estimation

1) Amplitude Estimation: The SM [9] estimates the global TWA amplitude as the squared root of the alternant power, measured as the difference between the averaged power spectrum at 0.5 cpb and the spectral noise level

$$v_l[p] = 2\sqrt{z_l[p] - m_l}, \quad V_l = \sqrt{Z_l - m_l} = \operatorname{RMS}(v_l[p]). \quad (30)$$

In complex demodulation based methods, the amplitude in each series is demodulated as

$$v_l[p] = 2e^{-j\pi l} (y_l[p] * h_{\text{hpf}}[l]). \quad (31)$$

The aggregate value is computed as $V_l = \sum_p |v_l[p]|$ in [22] and as $V_l = \operatorname{RMS}(v_l[p])$ in KLCD [27].

In the rest of STFT-based methods (PM, PT, Student tests), no amplitude estimator is given. However, it is straightforward to derive an estimator based on the STFT: $v_l[p] = 2Y_w[p, l]/\sum_i w[i]$ and $V_l = \operatorname{RMS}(v_l[p])$ from the statistics (14), (17), (19) and (21).

Assuming a constant value for the TWA in the repolarization interval, Burattini *et al.* [25] propose the following beat-to-beat amplitude estimator for the CM

$$V_i = 2 \frac{\sum_{n=0}^{N-1} x_{\text{med}}^2[n]}{\sum_{n=0}^{N-1} |x_{\text{med}}[n]|} \cdot |y_i - 1| = K \cdot |y_i - 1|. \quad (32)$$

In the MMA method, $z_l[p]$ and Z_l are, respectively, individual and global amplitude estimators.

The LLR method proposes the MLE under the assumption of Laplacian noise for estimating the alternans amplitude. The individual estimators are given by twice the median filtered complex demodulated series (29). The global TWA amplitude can be quantified as $V_l = \operatorname{RMS}(v_l[p])$.

The global TWA amplitude V_l is, thus, computed either as an averaged amplitude across the ST-T complex or as the maximum amplitude. When averaging, noise reduction is achieved at the expense of a certain underestimation of the measured amplitude.

2) Waveform Estimation: Since the first TWA observations, it is well known that alternans is not uniformly distributed along the ST-T complex. The characterization of TWA waveform, though still little studied in the TWA literature, might be clinically relevant. Some of the cited works [9], [22] give examples of TWA distributions. Recently, some studies have shown that TWA morphology may indicate ventricular tachycardia inducibility [63] and the location of alternating sources [52].

The ability to estimate the TWA morphology depends on both data reduction and analysis schemes. Information lost in the data reduction stage cannot be recovered even in the case of ideal analysis, as suggested by (3). Thus, methods reducing each beat to a single coefficient (see Table II) cannot be used for waveform estimation.

When the performed data reduction is equivalent to decimation (SM, CD, CF, PM, MMA and LLR), the $v_l[p]$ are direct estimates of TWA amplitude at several instants within the ST-T complex. Strictly speaking, $v_l[p]$ is an estimator of the decimated TWA waveform. The alternant signal $a_l[n]$ at its original sampling rate can be obtained by interpolation of $v_l[p]$. In the SM, only the absolute value of the distribution $|a_l[n]|$ can be obtained as the $v_l[p]$ (30) do not preserve the alternans phase.

In reduction schemes based on linear transforms (KLT methods), the $v_l[p]$ show the TWA distribution in the transformed domain. As suggested by (3), the TWA waveform can be reconstructed by adequately combining the $v_l[p]$, provided that the relative alternans sign/phase between series is preserved. In KLCD [27], the alternant waveform was estimated as the inverse KLT of $v_l[p]$, i.e., $\mathbf{a}_l = \mathbf{T} \mathbf{v}_l$.

E. TWA Analysis: Discussion and Examples

The discussion in this section is complemented by examples in real and simulated ECG records. They have been selected to illustrate some of the discussed aspects, and do not intend to serve as validation. We selected one signal (lead V2) digitally recorded with $F_s = 1000$ Hz, and resolution of $0.6 \mu\text{V}$ during a coronary angioplasty intervention. Other details about the dataset can be found in [52]. The duration of the signal is of 6 min. 22 s. (6:22), with a total of 482 beats. The balloon was inflated at time 0:30, and released at 5:24. A TWA episode is present from 4:00 to 5:30. This was visually checked in the raw ECG and by representing superposed beats.

This real ECG (Sig1) and two simulated signals were used in the examples. The simulated signal Sig2 is built from Sig1, where four ectopic beats recorded in the same patient were inserted at times 1:18, 2:35, 4:16, and 4:55. The two first are simulated before the TWA episode and the other two within alternans. From the last two, one breaks the TWA phase (i.e., ABXAB, where A,B represent alternating beats and X the ectopic beat) and the other does not break it (i.e., ABXBA). Another signal (Sig3) was synthesized by adding Gaussian noise with standard deviation of $50 \mu\text{V}$ in the band dc-20 Hz to the

real ECG in two 50-beat intervals, one before (from 1:57 until 2:35) and the other during TWA (from 3:56 until 4:36).

The same preprocessing stage was applied to the signals for all the methods, consisting on QRS detection, baseline rejection (cubic splines interpolation), ST-T segmentation (320-ms segments), alignment and column-wise filtering of the segment matrix (20-Hz cutoff frequency). As data reduction stage, decimation by $Q = 8$ ($P = 40$) was used for STFT-based and nonlinear filtering methods, while the maximum of T wave was selected for the sign-counting methods.

1) *STFT-Based Methods*: It has been shown that the detection statistics of methods based on periodogram, complex demodulation, Poincaré maps distance, periodicity transform and Student tests are monotonically related to the STFT of the beat-to-beat series at 0.5 cpb and, therefore, equivalent to the statistic $z_l[p] = |Y_w[p, l]|$. The differences between the approaches reside mainly in the shape and length of the analysis window $w[i]$.

The high-pass filter equivalence given by (7) can help to understand the effect of the analysis window in the detection performance. The filter should preserve the alternant component in each series, tracking its dynamic changes while rejecting as much noise as possible. We find, therefore, the classical tradeoff between tracking and denoising capabilities.

Short filters (low L) present better tracking of abrupt TWA changes and transient episodes than long filters (high L). On the other hand, the amount of smoothing performed on the beat-to-beat series by longer filters is greater, reducing the noise in the detection statistics and amplitude estimators. This tradeoff can be appreciated in Fig. 4(a) where the global detection statistic $Z_l = RMS(|Y_w[p, l]|) / \sum_i w(i)$ is represented for the signal Sig1, using Hanning analysis windows of lengths $L = 8, 32$ and 128 beats. Normalization by $\sum_i w(i)$ allows to compare different windows regardless of their scale and length. The smoothing effect of the 128-beat window does not allow a correct tracking of the transient TWA episode. However, the noise in Z_l (or V_l) is reduced with respect to the shorter windows. The 8-beat window results in noisy statistics, making difficult the work of the detection decision rule. In this case, the 32-beat window achieves a good compromise between tracking and denoising.

The assumption of stationarity within a 128-beat interval has been considered by Verrier *et al.* as one of the limitations of the SM in comparison to CD, as it is commonly practiced [36]. However, this limitation is attributable to the selected parameters rather than to the method itself. The kernel of the SM algorithm could track transient TWA episodes as well as the CD if the SM analysis window were the same as the effective duration of the CD impulse response, as it is illustrated in Fig. 4(b), where the statistic of CD in [22] (which uses an IIR filter with an effective length of 30 beats) shows similar tracking and noise characteristics as a 32-point periodogram (either standard or Hanning windowed).

In [32], it was also shown that the STFT at 0.5 cpb is the GLRT detector for TWA in stationary Gaussian noise, matched to TWA episodes with shape and duration given by the analysis window. This indicates that, from a detection point of view, the length of the window should be in the order of the expected episode length.

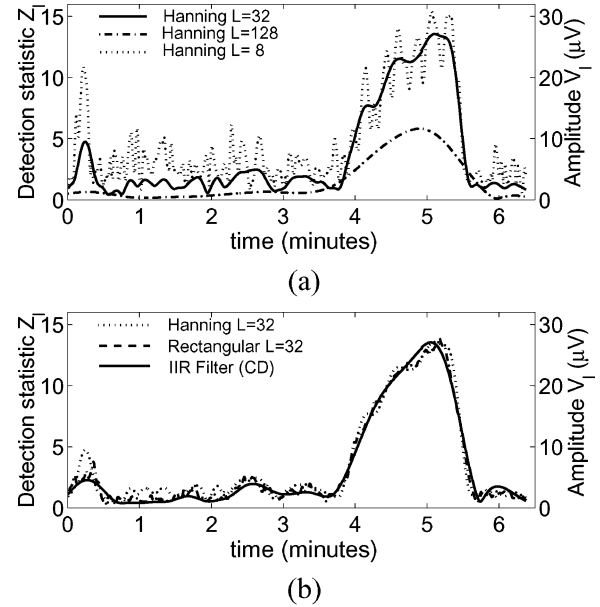


Fig. 4. STFT-based detection statistic Z_l applied to Sig1 with different analysis windows. The scale at the right represents the estimated amplitude V_l . (a) Hanning windows of different lengths. (b) Hanning and rectangular windows with $L = 32$, and CD method with the IIR filter used in [22].

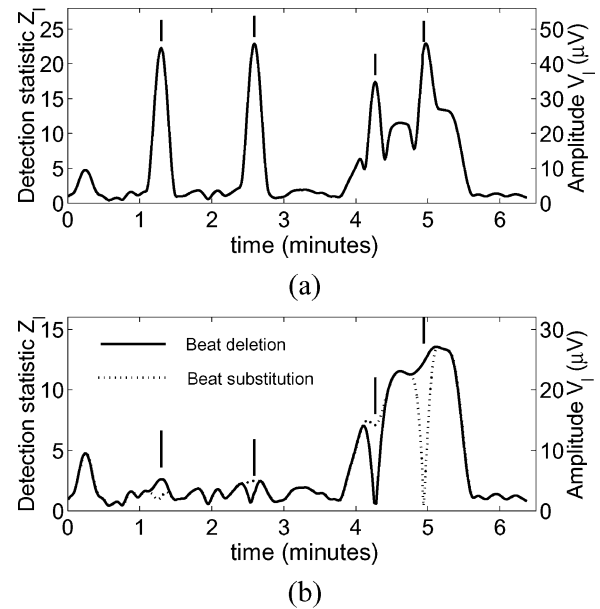


Fig. 5. Performance of the 32-beat hanning window STFT method applied to Sig2. Vertical lines indicate the positions of ectopic beats. (a) Without beat rejection. (b) With anomalous beat deletion (solid) and substitution (dotted).

Another remarkable aspect is the effect of impulsive artifacts in the beat-to-beat series. As an effect of linear filtering, the impulse energy will be spread at the output according to the impulse response. This disturbs detection and estimation in a neighborhood of L beats, as it can be seen in Fig. 5(a). Hence the importance of rejecting anomalous beats in the preprocessing stage before any linear filtering. In Fig. 5(b), the effect of anomalous beat deletion and substitution is exposed. Note that when an ectopic beat occurs during TWA, the best strategy depends on the phase behavior of the premature beat. Deletion is to be preferred if the anomalous beat produces a TWA phase

change, while substitution by a template beat works better when the phase is not broken by the ectopic beat. Both types of behavior have been observed in premature beats [63].

The shift parameter D defines the rate at which the detection statistic and amplitude estimate are computed. A running analysis window allows a beat-to-beat sampling of the TWA evolution (as shown in the figures of this paper). Some methods are presented in the literature following nonoverlapping ($D = L$) [28] or partial overlapping ($D = L/2$) [26] schemes. The SM is defined on a block by block basis ($D = L$), but a sliding window analysis can also be used as in [64] ($L = 64$, $D = 4$). Anyhow, the resolution of the method is determined by the effective filter duration L , rather than by the output rate defined by D . Overlap introduces correlation between consecutive detection statistics or estimates. The main benefits of using very overlapped windows (small D) is the better representation of TWA evolution, allowing the accurate location of the episode onsets, peaks and ends.

Although the detection statistic design has a great incidence in the analysis performance (time resolution, tracking of sudden changes, accuracy, robustness, . . .), the sensitivity and robustness of a detector also depend on the decision rules.

In CD, PM and PT, Z_l is compared with a fixed threshold. In contrast, the decision rules in the SM and the t tests allow adaptations to changing noise conditions. Equations (10), (19), and (21) reflect their equivalent thresholds. They depend on the estimated characteristics of the noise in the observed data: m_l and s_l measured in a spectral window for the SM and the pooled standard deviations S_l and s_l^Δ for the standard and paired t tests. Since s_l^Δ only accounts for the variability of the even-odd differences, the paired t test remains unaffected by slow drifts in the beat-to-beat series, unlike the standard t test. In the three cases, the required significance level can be set by adjusting the parameter γ .

The example in Fig. 6, where Sig3 is analyzed, exhibits how changes in the noise level affect Z_l and V_l and how the use of variant thresholds allows to discriminate between alternans and noise even if the alternant component quantified by Z_l is the same. This is clearly not possible using a fixed threshold. In [27], [62], the CD was used with an adaptive threshold set at a constant amount above the baseline of the statistic Z_l measured in non alternant signal excerpts. This strategy helped to reduce the number of false positives for a given sensitivity.

2) *Sign Change Counting Methods*: The Rayleigh test and CM use statistics based on the count of sign changes. The analysis of the zero-crossings of a signal has been used for spectral analysis [65]. To obtain reliable results, the signal must have a dominant frequency (the alternant component in our case) and a high signal-to-noise ratio [65]. Thus, the presence of other high amplitude components such as respiration, baseline wander or slow physiological variations can seriously degrade the performance of these methods. Hence the need of rejecting the respiration component in the CM (see Section IV-A).

The performance of the detection statistic (22) depends on the window length. The use of short counting windows (as $L = 7$ in CM) allows the detection of extremely brief TWA episodes, making possible its application to short ECG recordings. However, the shorter the window, the greater is the probability that a random sequence follows the required pattern, producing false

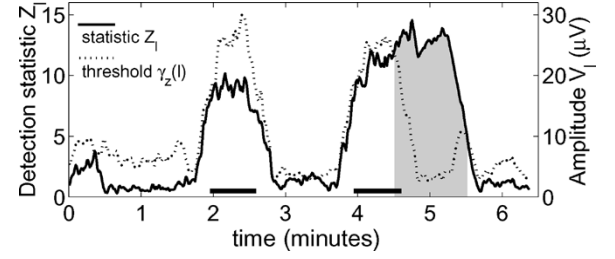


Fig. 6. Detection statistic of the STFT (using a 32-beat rectangular window) in the signal Sig3 (solid), and threshold $\gamma_l = \sqrt{m_l} + \gamma s_l$ (with $\gamma = 3$) proposed in the SM [9] (dotted). Horizontal lines mark the intervals with added noise. The shaded area indicates TWA detection.

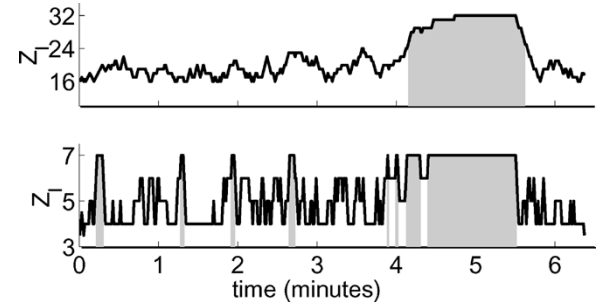


Fig. 7. Sign-counting methods applied to Sig1. Detection statistic (22) for $L = 32$ (top panel) and $L = 7$ (bottom panel). Shaded areas indicate TWA detection with thresholds $\gamma_z(l) = 25$ (top) and $\gamma_z(l) = 7$ (bottom).

detections, as those shown in Fig. 7 (bottom panel). This fact, together with the sensitivity to nonalternant components, explain the lack of robustness of the CM found in some simulation studies [27]. Longer windows (as $L = 32$ in [30]) assure greater robustness at the cost of requiring longer duration for detecting episodes (see top panel of Fig. 7).

Equation (23) emphasizes the interpretation of these methods as the STFT of the sign series. The sign nonlinearity limits the effect of outliers (impulsive noise, ectopic beats, . . .) in the detection statistic, in contrast with STFT-based methods. However, amplitude information is lost in the sign signal. In the Rayleigh test method, there is no amplitude estimator, while the CM uses a non sign-based estimator (32).

3) *Nonlinear Filtering Methods*: The main characteristic of these methods is their intrinsic robustness to outliers and impulsive noise in the beat-to-beat series.

In MMA, when differences between beats are small, (25) behaves linearly, and the statistic (26) is the result of high-pass linear filtering of the beat-to-beat series with the transfer function

$$H_{\text{hpf}}(z) = \frac{1}{8} z^{-2} \frac{1 - z^{-1}}{1 - \frac{7}{8} z^{-2}} \quad (33)$$

or equivalently, $z_l[p] = |Y_w[p, l]|$, with $w[l] = h_{\text{hpf}}[-i](-1)^i$. However, the nonlinearity (25) limits the effect of abrupt changes, artifacts and anomalous beats in the statistics and estimators. Fig. 8 illustrates the behavior of the MMA and its STFT-based counterpart (removing the nonlinearity). In signals Sig1 and Sig3, there are no abrupt changes in the beat-to-beat series, and the MMA works mainly as a linear filter. In contrast,

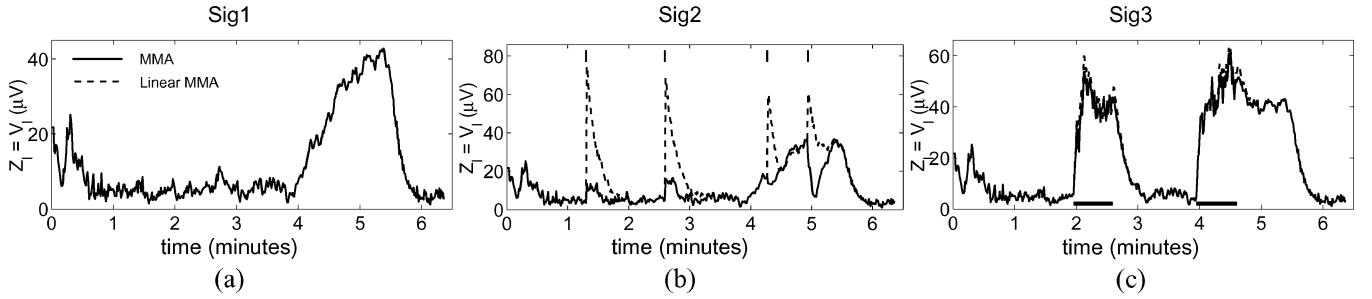


Fig. 8. MMA method applied to signals Sig1 (a), Sig2 (b) and Sig3 (c). Result of applying the MMA method as described in [31] (solid) and ignoring the nonlinearity (25) (dashed). Vertical lines in (b) and horizontal lines in (c) indicate, respectively, the location of ectopic beats and added noise intervals.

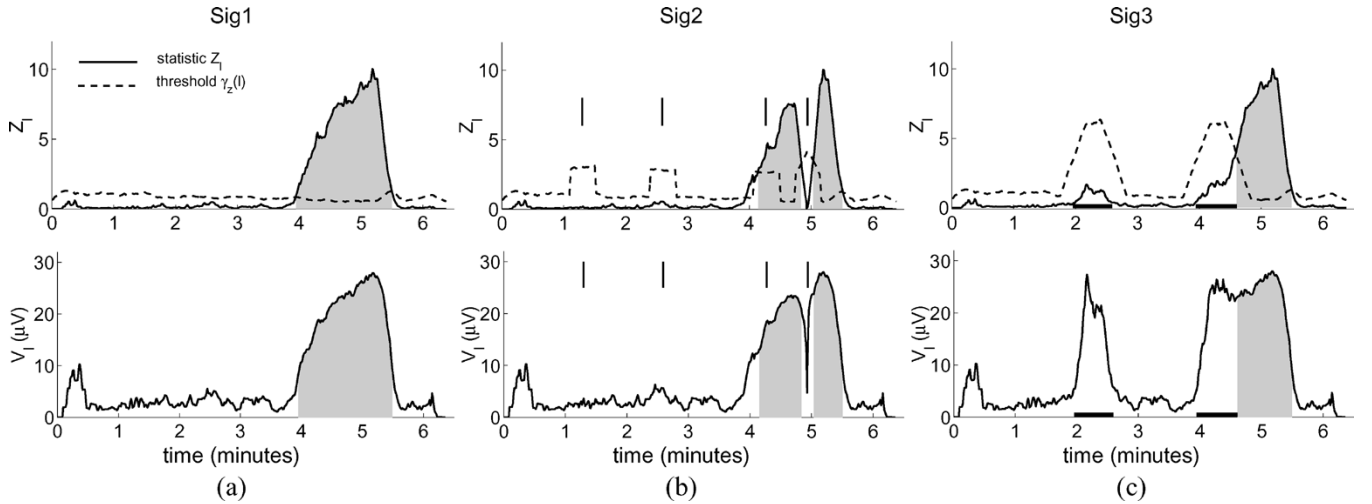


Fig. 9. LLR method applied to signals Sig1 (a), Sig2 (b) and Sig3 (c). Top panels show the LLR detection statistic Z_l (solid) and the variant threshold $\gamma_Z(l) = \gamma \sigma_l$ (with $\gamma = 0.1$) (dashed). Bottom panels show the eye-estimated amplitude (29). Vertical lines in (b) and horizontal lines in (c) are markers of ectopic beats and added noise intervals. Shaded areas indicate TWA detection.

when applied to Sig2, the MMA is virtually unaffected by ectopics, unlike the linear filter. The notch observed in the detection statistic is not due to the anomalous beat, but to the phase change in TWA provoked by the last ectopic beat.

The GLRT in the LLR (28) has been derived for Laplacian noise, which is a heavy-tailed distribution. As a consequence, the detection statistics and amplitude estimators are more robust to outliers than linear filtering methods. Note that $z_l[p]$ (28) takes the form of the STFT $Y_w[p, l]$ (6) with a rectangular window, where some extreme elements are discarded. The estimator $v_l[p]$ (29) is, in fact, a median-based version of the CD estimator (31).

The nonstationary version of LLR [33] allows the adaptation of the decision threshold to changes in the noise standard deviation, similarly to (19) and (21).

Fig. 9 shows the LLR detection statistic Z_l (28) and amplitude estimate V_l in signals Sig1 [Fig. 9(a)], Sig2 [Fig. 9(b)], and Sig3 [Fig. 9(c)]. The adaptive threshold $\gamma_Z(l) = \gamma s_l$ for $\gamma = 0.1$ is also shown.

According to the simulations in [31]–[33], nonlinear methods perform better than linear ones when faced with ectopic beats, abrupt changes, artifacts and heavy-tailed physiological noise, thus opening a promising line of robust detectors.

V. VALIDATION OF TWA METHODS

The aim of this section is just to draw attention to some aspects of validation that have not usually been taken into account. The development of suitable guidelines for TWA methods validation is, though, beyond the scope of this paper.

When referring to validation of TWA methods, we can distinguish between methodological validation (i.e., the quantification of the detection power and the estimation accuracy of the method) and clinical validation (which quantifies the adequateness of TWA as a risk stratifying measure). It is desirable to evaluate the method performance before using it to extract clinical conclusions.

The main problem for the methodological validation is the absence of a gold standard for TWA analysis. The existence of TWA validation databases annotated by human experts would be desirable. A big difficulty resides in the fact that TWA is often not visible due to its low amplitude (sometimes below the noise level). This hurdle could be overcome in the next years with the help of computerized analysis and visualization tools.

Some authors use a mixed validation: in [42], the SM and the CD were compared in terms of their ability to predict the result of the electrophysiologic test. The problem with this procedure is in that there is no way to know if a low

stratifying sensitivity/specificity is due to the errors of the analysis method or just to a lack of sensitivity/specificity of the clinical parameter.

In other cases, a new method is validated by correlating their results with those of the SM, i.e., using the SM as [28]. This procedure allows to test if a new method achieves a performance similar to a previously validated one, but does not allow any conclusion about the discordances between both methods.

The most common way of performance assessment is by means of simulation studies where TWA parameters (location, amplitude, duration, waveform) are known *a priori* [24], [26], [27], [29]–[33], [48], [53], [58], [62], [66]. Two aspects may influence their reliability: the degree of realism of the simulated signals (including the background ECG, TWA, and noise terms) and the possible overfit of the simulation to the method's underlying model.

We can find simulations with different degrees of realism in the literature. A synthesized alternating waveform is usually added to the ST-T complexes of a simulated noisy ECG. The background ECG is usually built as the repetition of a single noiseless beat (either synthetic [24], [31], [48], [53] or extracted from a real ECG [26], [27], [29], [30], [32], [58], [66]). One drawback of these approaches is that they do not consider physiological variability which can mask TWA in real recordings. Some of them scale the waveforms simulating heart rate variability [24], [31], [48]. Computer generated noise is added to the background ECG in [24], [26], [27], [29], [30], [32], [48] to test the performance in different levels of noise. A more realistic approach is to add recorded physiological noise as in [27], [32], where the MIT-BIH noise stress database was used. Finally, other settings [33], [58], [62] add simulated alternans to real nonalternant ECG recordings, with their own noise and physiological variability. These simulations provide very realistic results since neither the background ECG nor the noise terms are simulated.

As it has been shown in Section IV-E, the use of an analysis method with a parameter set has implications in the characteristics of TWA and noise that the method can cope with. Hence, overfitting between the parameters of the simulation (TWA episode duration, waveform, noise distribution, and stationarity, ...) and those of the analysis could yield biased results and should, therefore, be avoided.

VI. CONCLUSION

Two decades of computerized TWA analysis techniques have been revisited in this work and a three-stage unified framework has been proposed to dissect and analytically study the different methods. This framework has allowed us to find an analytical close relation between several methods regarded as markedly distinct in the literature, and also to isolate the principles of TWA detection and estimation from other auxiliary procedures and parameters.

The preprocessing stage is necessary to condition the signal for analysis. Its requirements are very dependent on the acquisition conditions, but also on the robustness of the subsequent stages.

Some linear data reduction schemes decrease the computational load by removing redundancy and undesired components. Their effect in the ECG is that of a linear time-variant periodic filter. Other methods use nonlinear schemes to extract relevant features of repolarization.

The core of the TWA methods lies in the detection and estimation substages. We have shown that most methods (including the most widely used SM and CD) are grounded in the short-time Fourier transform of the beat-to-beat series. The differences in performance among these methods can be explained on one hand by the characteristics of the analysis window, and on the other hand by the adaptation of the decision rule to changes in the noise characteristics. A second category gathers sign-change counting methods. The main drawback of these methods is their sensitivity to the presence of high amplitude nonalternant components. Finally, two recently proposed methods (MMA and LLR) form at the moment the category of nonlinear filtering methods. These are intrinsically robust to outliers or impulsive noise and have shown to perform better than linear methods in physiological noise.

REFERENCES

- [1] H. E. Hering, "Experimentelle studien an Säugetieren über das Elektrokardiogram," *Zeitschrift für experimentelle Pathologie und Therapie*, no. 7, pp. 363–378, 1909.
- [2] T. Lewis, "Notes upon alternation of the heart," *Quart. J. Med.*, no. 4, pp. 141–144, 1910.
- [3] W. W. Hamburger, L. N. Katz, and O. Saphir, "Electrical alternans: a clinical study with a report of two necropsies," *JAMA*, no. 106, pp. 902–905, 1936.
- [4] H. H. Kalter and M. L. Schwartz, "Electrical alternans," *N. Y. State J. Med.*, no. 1, pp. 1164–1166, 1948.
- [5] P. J. Schwartz and A. Malliani, "Electrical alternation of the T-wave: clinical and experimental evidence of its relationship with the sympathetic nervous system and with the long Q-T syndrome," *Am. Heart J.*, vol. 89, no. 1, pp. 45–50, 1975.
- [6] D. R. Adam, S. Akselrod, and R. J. Cohen, "Estimation of ventricular vulnerability to fibrillation through T-wave time series analysis," *Comput. Cardiol.*, vol. 8, pp. 307–310, 1981.
- [7] D. R. Adam, A. O. Powell, H. Gordon, and R. J. Cohen, "Ventricular fibrillation and fluctuations in the magnitude of the repolarization vector," *Comput. Cardiol.*, vol. 9, pp. 241–244, 1982.
- [8] D. R. Adam, J. M. Smith, S. Akselrod, S. Nyberg, A. O. Powell, and R. J. Cohen, "Fluctuations in T-wave morphology and susceptibility to ventricular fibrillation," *J. Electrocardiol.*, vol. 17, pp. 209–218, 1984.
- [9] D. S. Rosenbaum, L. E. Jackson, J. M. Smith, H. Garan, J. N. Ruskin, and R. J. Cohen, "Electrical alternans and vulnerability to ventricular arrhythmias," *N. Engl. J. Med.*, vol. 330, no. 4, pp. 235–241, 1994.
- [10] N. A. Estes III, G. Michaud, D. P. Zipes, N. El-Sherif, F. J. Venditti, D. S. Rosenbaum, P. Albrecht, P. J. Wang, and R. J. Cohen, "Electrical alternans during rest and exercise as predictors of vulnerability to ventricular arrhythmias," *Am. J. Cardiol.*, no. 80, pp. 1314–1318, 1997.
- [11] T. Kwan, A. Feit, M. Alam, E. Afflu, and L. T. Clark, "ST-T alternans and myocardial ischemia," *Angiology*, vol. 50, no. 3, pp. 217–222, 1999.
- [12] R. L. Verrier, B. D. Nearing, G. MacCallum, and P. H. Stone, "T-wave alternans during ambulatory ischemia in patients with stable coronary disease," *Ann. Noninvasive Electrocardiol.*, pt. 1, vol. 1, no. 2, pp. 113–120, 1996.
- [13] W. Zareba, A. J. Moss, S. Le Cessie, and W. Hall, "T wave alternans in idiopathic long QT syndrome," *J. Am. Coll. Cardiol.*, no. 23, pp. 1541–1546, 1994.
- [14] R. L. Verrier, B. D. Nearing, M. T. LaRovere, G. D. Pinna, M. A. Mittelman, J. T. Bigger, and P. J. Schwartz, "Ambulatory electrocardiogram-based tracking of T wave alternans in postmyocardial infarction patients to assess risk of cardiac arrest or arrhythmic death," *J. Cardiovasc. Electrophysiol.*, vol. 14, no. 7, pp. 705–711, 2003.
- [15] G. Turitto and N. El-Sherif, "Alternans of the ST segment in variant angina. incidence, time course and relation to ventricular arrhythmias during ambulatory electrocardiographic recording," *Chest*, vol. 93, pp. 587–591, 1988.

- [16] K. Adachi, Y. Ohnisch, T. Shima, K. Yamashiro, A. Takei, N. Tamura, and M. Yokoyama, "Determinant of microvolt-level T-wave alternans in patients with dilated cardiomyopathy," *J. Am. Coll. Cardiol.*, vol. 34, no. 2, pp. 374–380, 1999.
- [17] J. M. Smith, E. A. Clancy, C. R. Valeri, J. N. Ruskin, and R. J. Cohen, "Electrical alternans and cardiac electrical instability," *Circulation*, vol. 77, no. 1, pp. 110–121, 1988.
- [18] G. Turitto, E. B. Caref, G. El-Attar, M. Helal, A. Mohamed, R. P. Pedalino, and N. El-Sherif, "Optimal target heart rate for exercise-induced T-wave alternans," *Ann. Noninvasive Electrocardiol.*, vol. 6, no. 2, pp. 123–128, 2001.
- [19] S. Weber, H. Tillmanns, and B. Waldecker, "Prevalence of T wave alternans in healthy subjects," *Pacing Clin. Electrophysiol.*, vol. 26, no. 1p1, pp. 49–51, 2003.
- [20] W. J. Kop, D. S. Krantz, B. D. Nearing, J. S. Gottdiener, J. F. Quigley, M. O'Callahan, A. A. DelNegro, T. D. Friebling, P. Karasik, S. Suchday, J. Levine, and R. L. Verrier, "Effects of acute mental stress and exercise on T-wave alternans in patients with implantable cardioverter defibrillators and controls," *Circulation*, vol. 109, pp. 1864–1869, 2004.
- [21] B. D. Nearing, A. H. Huang, and R. L. Verrier, "Dynamic tracking of cardiac vulnerability by complex demodulation of the T wave," *Science*, no. 252, pp. 437–440, 1991.
- [22] B. D. Nearing and R. L. Verrier, "Personal computer system for tracking cardiac vulnerability by complex demodulation of the T wave," *J. Appl. Physiol.*, vol. 74, no. 5, pp. 2606–2612, 1993.
- [23] L. Burattini, W. Zareba, J. P. Couderc, E. L. Titlebaum, and A. J. Moss, "Computer detection of nonstationary T-wave alternans using a new correlative method," *Comput. Cardiol.*, vol. 24, pp. 657–660, 1997.
- [24] L. Burattini, "Electrocardiographic T Wave Alternans Detection and Significance," Ph.D. dissertation, University of Rochester, Rochester, NY, 1998.
- [25] L. Burattini, W. Zareba, and A. J. Moss, "Correlation method for detection of transient T-wave alternans in digital Holter ECG recordings," *Ann. Electrocardiol.*, vol. 4, no. 4, pp. 416–426, 1999.
- [26] P. Laguna, M. Ruiz, G. B. Moody, and R. G. Mark, "Repolarization alternans detection using the KL transform and the beatquency spectrum," *Comput. Cardiol.*, vol. 23, pp. 673–676, 1996.
- [27] J. P. Martínez, S. Olmos, and P. Laguna, "Simulation study and performance evaluation of T-wave alternans detectors," in *Proc. 22nd Ann. Int. Conf. IEEE Engineering in Medicine and Biology Soc. (CD-ROM)*, 2000.
- [28] P. Strumillo and J. Ruta, "Poincaré mapping for detecting abnormal dynamics of cardiac repolarization," *IEEE Eng. Med. Biol. Mag.*, vol. 21, no. 1, pp. 62–65, 2002.
- [29] T. Srikanth, D. Lin, N. Kanaan, and H. Gu, "Estimation of low level alternans using periodicity transform—simulation and european ST/T database results," in *Proc. 24th Ann. Int. Conf. IEEE Engineering in Medicine and Biology Soc.*, 2002, pp. 1407–1408.
- [30] —, "Presence of T wave alternans in the statistical context—a new approach to low amplitude alternans measurement," *Comput. Cardiol.*, vol. 29, pp. 681–684, 2002.
- [31] B. D. Nearing and R. L. Verrier, "Modified moving average analysis of T-wave alternans to predict ventricular fibrillation with high accuracy," *J. Appl. Physiol.*, no. 92, pp. 541–549, 2002.
- [32] J. P. Martínez and S. Olmos, "A robust T-wave alternans detector based on the GLRT for Laplacian noise distribution," in *Proc. Comput. Cardiol. 2002*, Piscataway, NJ, 2002, pp. 677–680.
- [33] —, "Detection of T wave alternans in nonstationary noise: a GLRT approach," in *Proc. Computers in Cardiology 2003*, Piscataway, NJ, 2003, pp. 161–164.
- [34] D. E. Euler, "Cardiac alternans: mechanisms and pathophysiological significance," *Cardiovasc. Res.*, vol. 42, pp. 583–590, 1999.
- [35] M. V. Walker and D. S. Rosenbaum, "Repolarization alternans: implications for the mechanism and prevention of sudden cardiac death," *Cardiovasc. Res.*, vol. 57, pp. 599–614, 2003.
- [36] R. L. Verrier, W. Zareba, and B. D. Nearing, "T-wave alternans monitoring to assess risk for ventricular tachycardia and fibrillation," in *Non-invasive Electrocardiology. Clinical Aspects of Holter Monitoring*, A. J. Moss and S. Stern, Eds. London, U.K.: Saunders, 1996, ch. 25, pp. 445–464.
- [37] D. S. Rosenbaum, P. Albrecht, and R. J. Cohen, "Predicting sudden cardiac death from T wave alternans of the surface electrocardiogram: promise and pitfalls," *J. Cardiovasc. Electrophysiol.*, vol. 7, no. 11, pp. 1095–1111, 1996.
- [38] E. Locati, L. Burattini, and W. Zareba, "Identification of T-wave alternans: review of methods and clinical perspectives," in *Rhythm Control: From Cardiac Evaluation to Treatment*, E. Adornato, Ed. Roma: Edizioni Luigi Pozzi, 1998, pp. 173–184.
- [39] M. Takagi and J. Yoshikawa, "T wave alternans and ventricular tachyarrhythmia risk stratification: a review," *Indian Pacing Electrophysiol. J.*, vol. 3, no. 2, pp. 67–73, 2003.
- [40] Q. Pham, K. J. Quan, and D. S. Rosenbaum, "T-wave alternans: marker, mechanism, and methodology for predicting sudden cardiac death," *J. Electrocardiol.*, vol. 36, pp. 75–81, 2003.
- [41] W. Zareba, J. P. Couderc, and A. J. Moss, "Automatic detection of spatial and temporal heterogeneity of repolarization," in *Dispersion of Ventricular Repolarization: State of the Art*, S. B. Olsson, S. Yuan, and J. P. Amlie, Eds. New York: Futura, 2000, ch. 6, pp. 85–107.
- [42] D. S. Rosenbaum, X. Fang, and J. A. Mackall, "How to detect ECG T-wave alternans in patients at risk for sudden cardiac death," *J. Am. Coll. Cardiol.*, vol. 25, no. 2, p. 409A, 1995.
- [43] S. H. Hohnloser, T. Klingenheben, L. Yi-Gang, M. Zabel, J. Peetermans, and R. J. Cohen, "T-wave alternans as a predictor of recurrent ventricular tachyarrhythmias in ICD recipients: prospective comparison with conventional risk markers," *J. Cardiovasc. Electrophysiol.*, vol. 9, pp. 1258–1268, 1998.
- [44] M. R. Gold, D. M. Bloomfield, K. Anderson, N. El Sherif, D. Wilber, E. Kaufman, M. Greenberg, and D. Rosenbaum, "A comparison of T-wave alternans, signal averaged electrocardiography and programmed ventricular stimulation for arrhythmia risk stratification," *J. Am. Coll. Cardiol.*, no. 36, pp. 2247–2253, 2000.
- [45] T. Klingenheben, M. Zabel, R. B. D'Agostino, R. J. Cohen, and S. H. Hohnloser, "Predictive value of T-wave alternans for arrhythmic events in patients with congestive heart failure," *Lancet*, vol. 356, pp. 651–652, 2000.
- [46] T. Ikeda, H. Saito, K. Tanno, H. Shimizu, J. Watanabe, Y. Ohnishi, Y. Kasamaki, and Y. Ozawa, "T-wave alternans as a predictor for sudden cardiac death after myocardial infarction," *Am. J. Cardiol.*, vol. 89, pp. 79–82, 2002.
- [47] B. D. Nearing, S. N. Oesterle, and R. L. Verrier, "Quantification of ischaemia induced vulnerability by precordial T wave alternans analysis in dog and human," *Cardiovasc. Res.*, vol. 28, pp. 1440–1449, 1994.
- [48] L. Burattini, W. Zareba, E. J. Rashba, J. P. Couderc, J. Konecki, and A. J. Moss, "ECG features of microvolt T-wave alternans in coronary artery disease and long QT syndrome patients," *J. Electrocardiol.*, vol. 31, pp. 114–120, 1998.
- [49] P. Stoica and R. Moses, *Introduction to Spectral Analysis*. Upper Saddle River, NJ: Prentice-Hall, 1997.
- [50] W. A. Sethares and T. W. Staley, "Periodicity transforms," *IEEE Trans. Signal Process.*, vol. 47, no. 11, pp. 2953–2964, Nov. 1999.
- [51] S. M. Kay, *Fundamentals of Statistical Signal Processing*. Upper Saddle River, NJ: Prentice-Hall, 1998, vol. II, Detection theory.
- [52] J. P. Martínez, S. Olmos, and P. Laguna, "T wave alternans and acute ischemia in patients undergoing angioplasty," in *Proc. Comput. Cardiol. 2002*, vol. 29, 2002, pp. 569–572.
- [53] B. D. Nearing, P. H. Stone, and R. L. Verrier, "Frequency-response characteristics required for detection of T-wave alternans during ambulatory ECG monitoring," *Ann. Noninvasive Electrocardiol.*, pt. 1, vol. 1, no. 2, pp. 103–112, 1996.
- [54] G. B. Moody and R. G. Mark, "Development and evaluation of a 2-lead ECG analysis program," *Comput. Cardiol.*, pp. 39–44, 1982.
- [55] N. V. Thakor, J. G. Webster, and W. J. Tompkins, "Estimation of QRS complex power spectrum for design of a QRS filter," *IEEE Trans. Biomed. Eng.*, vol. BME-31, no. 11, pp. 702–706, Nov. 1984.
- [56] L. Burattini, W. Zareba, J. P. Couderc, J. A. Konecki, and A. J. Moss, "Optimizing ECG signal sampling frequency for T-wave alternans detection," *Comput. Cardiol.*, vol. 25, pp. 721–724, 1998.
- [57] B.-U. Köhler, C. Hennig, and R. Orglmeister, "The principles of software QRS detection," *IEEE Eng. Med. Biol. Mag.*, vol. 21, no. 1, pp. 42–57, Jan./Feb. 2002.
- [58] S. M. Narayan and J. M. Smith, "Spectral analysis of periodic fluctuations in electrocardiographic repolarization," *IEEE Trans. Biomed. Eng.*, vol. 46, no. 2, pp. 203–212, Feb. 1999.
- [59] M. J. Lisenby and P. C. Richardson, "The beatquency domain: an unusual application of the fast Fourier transform," *IEEE Trans. Biomed. Eng.*, vol. BME-24, pp. 405–408, 1977.
- [60] S. Olmos, J. Garcia, R. Jané, and P. Laguna, "Truncated orthogonal expansions of recurrent signals: equivalence to a linear time-variant periodic filter," *IEEE Trans. Signal Process.*, vol. 47, no. 11, pp. 3164–3172, Nov. 1999.
- [61] —, "ECG signal compression plus noise filtering with truncated orthogonal expansions," *Signal Process.*, vol. 79, no. 1, pp. 97–115, Oct 1999.
- [62] J. P. Martínez, S. Olmos, and P. Laguna, "T wave alternans detection: a simulation study and analysis of the European ST-T database," *Comput. Cardiol.*, vol. 27, pp. 155–158, 2000.
- [63] S. M. Narayan, B. D. Lindsay, and J. M. Smith, "Demonstration of the proarrhythmic preconditioning of single premature extrastimuli by use of the magnitude, phase and distribution of repolarization alternans," *Circulation*, vol. 100, pp. 1887–1893, 1999.

- [64] E. S. Kaufman, J. A. Mackall, B. Julka, C. Drabek, and D. S. Rosenbaum, "Influence of heart rate and sympathetic stimulation on arrhythmogenic T wave alternans," *Am. J. Physiol. Heart Circ. Physiol.*, vol. 279, pp. H1248–H1255, 2000.
- [65] B. Kedem, "Spectral analysis and discrimination by zero-crossings," *Proc. IEEE*, vol. 74, no. 11, pp. 1477–1493, Nov. 1986.
- [66] R. Mrowka, H. Theres, A. Patzak, and G. Baumann, "Alternans-like phenomena due to filtering of electrocardiographic data," *Comput. Cardiol. 1998*, pp. 725–727, 1998.



Juan Pablo Martínez was born in Zaragoza, Aragon, Spain, in 1976. He received the M. Sc. degree in telecommunication engineering (with highest honors) from the University of Zaragoza (UZ), in 1999.

From 1999 to 2000 he was with the Department of Electronic Engineering and Communications, UZ, as a Research Fellow. Since 2000, he is as an Assistant Professor in the same Department. He is also involved as researcher with the Aragon Institute of Engineering Research (I3A), UZ. His

professional research activity lies in the field of biomedical signal processing, with main interest in signals of cardiovascular origin.



Salvador Olmos (A'01–M'03) was born in Valencia, Spain in 1969. He received the Industrial Engineering degree and the Ph.D. degree from the Polytechnic University of Catalonia, Catalonia, Spain, in 1993 and 1998, respectively.

He is currently an Associate Professor of Signal Processing and Communications in the Department of Electronics Engineering and Communications at Zaragoza University, Spain. From August 2000 to August 2001 he was with the Department of Electroscience, Lund University, Lund, Sweden,

supported by a postdoctoral research grant from Spanish Government. His professional research interests are in signal processing of biomedical signals.